

# Non-singlet QCD analysis of $F_2(x, Q^2)$ up to NNLO

M. Glück, E. Reya, C. Schuck

*Institut für Physik, Universität Dortmund  
D-44221 Dortmund, Germany*

## Abstract

The significance of NNLO (3-loop) QCD contributions to the flavor non-singlet sector of  $F_2^{ep}$  and  $F_2^{ed}$  has been studied as compared to uncertainties (different factorization schemes, higher twist and QED contributions) of standard NLO (and LO) QCD analyses. The latter effects turn out to be comparable in size to the NNLO contributions. Therefore the minute NNLO effects are unobservable with presently available (precision) data on non-singlet structure functions.

# 1 Introduction

In a recent publication [1] a next-to-next-to-leading order (NNLO) QCD analysis of  $F_2^{ep}(x, Q^2)$  and  $F_2^{ed}(x, Q^2)$  in the flavor non-singlet sector was presented. Here our purpose is to study the significance of the NNLO contribution as compared to other, possibly important, contributions such as redundant terms in the NLO analysis (which arise when the NLO evolved parton distributions are multiplied by the coefficient function), higher twist and QED contributions to NLO, and effects due to choosing different factorization schemes. In Sec. 2 we present the relevant theoretical expressions required for our analysis, and Sec. 3 contains the quantitative results. Our conclusions are summarized in Sec. 4.

## 2 Theoretical Formalism

The non-singlet (NS) parts of the structure functions  $F_2^{ep,d}(x, Q^2)$  for  $x > 0.3$ , where valence quark dominance is adopted, are, at LO, given by

$$F_2^{ep} = \frac{4}{9} x u_v + \frac{1}{9} x d_v \equiv \frac{5}{18} x q_{\text{NS},8}^+ + \frac{1}{6} x q_{\text{NS},3}^+ \quad (1)$$

$$F_2^{ed} = \frac{5}{18} x(u_v + d_v) \equiv \frac{5}{18} x q_{\text{NS},8}^+ \quad (2)$$

where  $d = (p + n)/2$  and  $q_{\text{NS},3}^+ = u_v - d_v$ . For  $x < 0.3$  one analyzes the genuine NS combination

$$F_2^{p-n} \equiv 2(F_2^{ep} - F_2^{ed}) = \frac{1}{3} x(u_v - d_v) + \frac{2}{3} x(\bar{u} - \bar{d}) \equiv \frac{1}{3} x q_{\text{NS},3}^+ \quad (3)$$

where now  $q_{\text{NS},3}^+ = u_v - d_v + 2(\bar{u} - \bar{d})$  since sea quarks cannot be neglected for  $x$  smaller than about 0.3. For definiteness we adopt for  $\bar{d} - \bar{u}$  the choice [2, 1]

$$x(\bar{d} - \bar{u})(x, Q_0^2) = 1.195x^{1.24}(1 - x)^{9.1}(1 + 14.05x - 45.52x^2) \quad (4)$$

at  $Q_0^2 = 4 \text{ GeV}^2$  which gives a good description of the Drell-Yan dimuon production data [3], but plays a marginal role in our analysis.

At NLO( $\overline{\text{MS}}$ ) the  $n$ -th Mellin moments of the above NS combinations of valence parton distributions, for brevity denoted by  $v^+$ , symbolically evolve according to the well known expression (see, e.g. [4, 5])

$$v^+(Q^2) = \{1 - (a - a_0)R_1\} (a/a_0)^{-P_{\text{NS}}^{(0)}/\beta_0} v^+(Q_0^2) \quad (5)$$

where  $R_1 = P_{\text{NS}}^{(1)+}/\beta_0 - (\beta_1/\beta_0^2)P_{\text{NS}}^{(0)}$  and  $a = a(Q^2) \equiv \alpha_s(Q^2)/4\pi$  with  $a_0 = a(Q_0^2)$ . The moments of the above NS structure functions  $F_2^{\text{NS}}$  are then given by

$$F_2^{\text{NS}}(Q^2) = \left[1 + aC_{2,\text{NS}}^{(1)}\right] v^+(Q^2) \quad (6)$$

and this expression is commonly compared with experiment. Inserting  $v^+(Q^2)$  from (5) into this equation one observes a *redundant*  $\mathcal{O}(a^2)$  contribution, i.e.  $-a(a - a_0)C_{2,\text{NS}}^{(1)}R_1$ , which in fact belongs to a NNLO analysis and is assumed to be small at NLO. If, however, one chooses to work to a NNLO (3-loop) accuracy, such a redundancy at NLO might become significant as compared to the full NNLO contribution. This will be investigated quantitatively below. Similarly, the choice of a factorization scheme, other than the  $\overline{\text{MS}}$  scheme used thus far, might imply larger differences than additional NNLO contributions in the  $\overline{\text{MS}}$  scheme. For example, in the deep inelastic scattering (DIS) factorization scheme [6, 4] the Wilson coefficient in (6) is absorbed into the parton distributions, i.e. into their evolutions in (5) with  $R_1 \rightarrow R_1^{\text{DIS}} = R_1 - C_{2,\text{NS}}^{(1)}$ :

$$v_{\text{DIS}}^+(Q^2) = \{1 - (a - a_0)R_1^{\text{DIS}}\} (a/a_0)^{-P_{\text{NS}}^{(0)}/\beta_0} v^+(Q_0^2) \quad (7)$$

and, instead of (6),  $F_2^{\text{NS}} = v_{\text{DIS}}^+$  at NLO.

Taking into account QCD 3-loop NNLO  $\alpha_s^3$  effects, one also has to consider QED LO  $\alpha$ -contributions which are of comparable size [7]. The latter can easily be implemented by changing the  $n$ -th moments of the NLO valence input distribution  $q_v(Q_0^2)$ ,  $q_v = u_v, d_v$ , in (5) according to

$$q_v(Q_0^2) \rightarrow (a/a_0)^{\frac{\alpha}{4\pi} \frac{\beta_1}{\beta_0^2} P^\gamma} \exp \left[ \frac{\alpha}{4\pi\beta_0} \left( \frac{1}{a} - \frac{1}{a_0} \right) P^\gamma \right] q_v(Q_0^2) \quad (8)$$

with  $\alpha \simeq \frac{1}{137}$  and  $P^\gamma = (e_q^2/C_F)P_{\text{NS}}^{(0)}$  where  $C_F = 4/3$ .

At NNLO( $\overline{\text{MS}}$ ) the evolution of  $v^+(Q^2)$  in (5) generalizes to

$$v^+(Q^2) = \{1 - (a - a_0)R_1 - \frac{1}{2}(a^2 - a_0^2)(R_2 - R_1^2) - a_0(a - a_0)R_1^2\}(a/a_0)^{-P_{\text{NS}}^{(0)}/\beta_0} v^+(Q_0^2) \quad (9)$$

with  $R_2 = P_{\text{NS}}^{(2)+}/\beta_0 - (\beta_1/\beta_0)R_1 - (\beta_2/\beta_0^2)P_{\text{NS}}^{(0)}$  and (6) becomes

$$F_2^{\text{NS}}(Q^2) = \left[1 + aC_{2,\text{NS}}^{(1)} + a^2C_{2,\text{NS}}^{(2)+}\right] v^+(Q^2). \quad (10)$$

Convenient expressions for the relevant 2-loop Wilson coefficient  $C_{2,\text{NS}}^{(2)+}$  can be found in [5] (eq. (A.2)) and for the 3-loop splitting function  $P_{\text{NS}}^{(2)+}$  in [8] (eq. (4.22), which can be easily Mellin-transformed using [9]). The strong coupling now evolves according to  $da/d\ln Q^2 = -\sum_{\ell=0}^2 \beta_\ell a^{\ell+2}$  where  $\beta_0 = 11 - 2f/3$ ,  $\beta_1 = 102 - 38f/3$  and  $\beta_2 = 2857/2 - 5033f/18 + 325f^2/54$ , which refers to the  $\overline{\text{MS}}$  renormalization scheme, and  $f$  denotes the number of active flavors. Here the redundant  $\mathcal{O}(a^3, a^4)$  contributions in (10) turn out to be marginal and do not influence our (fit) results. Furthermore, the running coupling  $a(Q^2)$  is appropriately matched at  $Q = m_b = 4.5$  GeV and  $Q = m_t = 175$  GeV. To obtain  $F_2^{\text{NS}}$  in the DIS factorization scheme at NNLO, the Wilson coefficient functions in (10) have to be absorbed into the parton distributions, i.e. into their evolutions in (9) with  $R_2 \rightarrow R_2^{\text{DIS}} = R_2 - 2C_{2,\text{NS}}^{(2)+} + (C_{2,\text{NS}}^{(1)})^2$ :

$$\begin{aligned} v_{\text{DIS}}^+(Q^2) &= \{1 - (a - a_0)R_1^{\text{DIS}} - \frac{1}{2}(a^2 - a_0^2) [R_2^{\text{DIS}} - (R_1^{\text{DIS}})^2] \\ &\quad - a_0(a - a_0)(R_1^{\text{DIS}})^2\} (a/a_0)^{-P_{\text{NS}}^{(0)}/\beta_0} v^+(Q_0^2) \end{aligned} \quad (11)$$

where  $R_1^{\text{DIS}}$  is as in the NLO-DIS expression (7) and, instead of (10), we now have  $F_2^{\text{NS}} = v_{\text{DIS}}^+$  at NNLO.

Since flavor NS structure functions are mainly related to the medium and large  $x$ -region, the relevant kinematic nucleon target mass (TM) corrections are always taken

into account according to [10]

$$\begin{aligned}
F_{2,\text{TM}}^{\text{NS}}(n, Q^2) &\equiv \int_0^1 x^{n-2} F_{2,\text{TM}}^{\text{NS}}(x, Q^2) dx = \\
&= \sum_{j=0}^2 \left( \frac{m_N^2}{Q^2} \right)^j \frac{(n+j)!}{j!(n-2)!} \frac{F_2^{\text{NS}}(n+2j, Q^2)}{(n+2j)(n+2j-1)} + \mathcal{O} \left( \left( \frac{m_N^2}{Q^2} \right)^3 \right) \quad (12)
\end{aligned}$$

where higher powers than  $(m_N^2/Q^2)^2$  are negligible for the relevant  $x < 0.8$  region, as can straightforwardly be shown by comparing (12) with the well known exact expression in Bjorken- $x$  space [10].

Despite the kinematic cuts ( $Q^2 \geq 4 \text{ GeV}^2$ ,  $W^2 \equiv (\frac{1}{x} - 1) Q^2 + m_N^2 \geq 10 \text{ GeV}^2$ ) used for our analysis, we also take into account higher twist (HT) corrections to  $F_2^{\text{NS}}$  via

$$v^+(x, Q^2) \rightarrow \left[ 1 + \frac{m_N^2}{Q^2} h(x) \right] v^+(x, Q^2) \quad (13)$$

in order to learn whether nonperturbative effects may still contaminate our perturbative analysis. Here we adopt the ansatz [11]

$$h(x) = a \left( \frac{x^b}{1-x} - c \right). \quad (14)$$

Notice that the input valence parton distributions  $v^+(x, Q_0^2)$  at LO [ $v^+(Q^2) = (a/a_0)^{-P_{\text{NS}}^{(0)}/\beta_0} v^+(Q_0^2)$ ], NLO and NNLO in the  $\overline{\text{MS}}$  as well as in the DIS scheme in eqs. (5)–(11) and (13) can and will be *different* in general.

Finally, Fermi motion and nuclear effects in the deuteron are strongly model dependent and will therefore not be considered here. They were, however, taken into account in [1, 11, 12] using the specific models cited there. Comparing these results with our valence distributions obtained and to be discussed below, as well as with other results where such effects have not been taken into account (e.g. [2]), shows that these effects do not change the quality of the QCD fits.

### 3 Quantitative results

In the present analysis we used the proton and deuteron data of BCDMS [13], NMC [14] and SLAC [15], as well as the proton data of H1 [16] and ZEUS [17] in the relevant  $x$ -regions discussed above which amount to 480 data points. The valence distributions have been parametrized at the input scale  $Q_0^2 = 4 \text{ GeV}^2$  as

$$x u_v(x, Q_0^2) = N_u x^{a_u} (1-x)^{b_u} (1 + A_u x^{c_u} + B_u x) \quad (15)$$

$$x d_v(x, Q_0^2) = N_d x^{a_d} (1-x)^{b_d} (1 + A_d x^{c_d} + B_d x) \quad (16)$$

with the normalizations  $N_u$  and  $N_d$  being fixed by  $\int_0^1 u_v dx = 2$  and  $\int_0^1 d_v dx = 1$ , respectively. The LO, NLO and NNLO fit results without HT contributions are summarized in Table 1. The standard NLO and NNLO fits refer to the  $\overline{\text{MS}}$  scheme according to eqs. (5), (6) and (9), (10), respectively. Our fit results for NNLO are compared in Fig. 1 with the data used. Except perhaps in LO, we obtained equally good and acceptable fits ( $\chi^2/\text{dof}$ ) in each perturbative order and scenario. As has been already noted previously [1, 12, 18, 19], a NNLO analysis in general results in a slightly smaller  $\alpha_s(m_Z^2)$  than in NLO. This is due to the fact that the higher the perturbative order the faster  $\alpha_s(Q^2)$  increases as  $Q^2$  decreases. In order to compensate for this increase, a NNLO fit is expected to result in a smaller value for  $\alpha_s(m_Z^2)$  than a NLO fit. Notice that the values of  $\alpha_s(m_Z^2)$  obtained in the usual perturbative NLO and NNLO fits in Table 1 are comparable to the ones in [1, 12, 18]. Repeating the NLO and NNLO fits in the DIS factorization scheme improves only marginally the global  $\overline{\text{MS}}$  fits ( $\chi^2$ ), and the QED  $\mathcal{O}(\alpha)$  contributions leave the original NLO( $\overline{\text{MS}}$ ) results practically unchanged as evident from Table 1.

On the other hand, the inclusion of higher twist contributions sizeably improves the fits, i.e., the value of  $\chi^2/\text{dof}$  as can be seen from Table 2 ( $\alpha_s(m_Z^2)$  is reduced as expected since the HT term takes care already of some of the  $Q^2$ -dependence of the data). In order to illustrate the relative significance of the (model dependent) HT corrections in (13), we have performed a fit for  $Q^2 \geq 4 \text{ GeV}^2$  and one for  $Q^2 \geq 10 \text{ GeV}^2$ , denoted by HT(10) in

Table 2. Clearly, HT effects become less important when the lower cut of  $Q^2$  is increased and the value of  $\chi^2$  increases, eventually approaching the larger values obtained by purely perturbative fits. Nevertheless it is remarkable that the fits for  $Q^2 \geq 4 \text{ GeV}^2$  and  $Q^2 \geq 10 \text{ GeV}^2$  are not significantly different as will be illustrated below (Fig. 2). For illustration we also show in Fig. 1 the NNLO results with HT effects included for  $Q^2 \geq 4 \text{ GeV}^2$ . The results for the  $Q^2 \geq 10 \text{ GeV}^2$  cut are not shown, since they are very similar to the ones for the  $Q^2 \geq 4 \text{ GeV}^2$  cut (dashed curves).

The actual relative size of our results can best be seen by comparing the various fit results with the pure QCD NLO fit, i.e. by considering the following ratios, depicted in Fig. 2, which are defined as follows. The effect of NNLO contributions can be visualized via  $r_{\text{NNLO}} = F_{2,\text{NNLO}}^{ep}/F_{2,\text{NLO}}^{ep}$  with the nominal NLO structure function given by (6) and the NNLO one by (10). Similarly,  $r_{\text{LO}}$  requires the usual  $F_{2,\text{LO}}^{ep}$  as given by (5) and (6) with  $R_1 \equiv 0$  and  $C_2^{(1)} \equiv 0$ . Furthermore  $r_{\text{NLO}}^{\text{DIS}} = F_{2,\text{NLO}}^{ep,\text{DIS}}/F_{2,\text{NLO}}^{ep}$  illustrates the effects of choosing the DIS factorization scheme instead of the  $\overline{\text{MS}}$  scheme, with the DIS structure function given by (7). Similarly, the definition of  $r_{\text{NNLO}}^{\text{DIS}}$  employs the DIS structure function in NNLO given by (11). Including the QED  $\mathcal{O}(\alpha)$  contributions to  $F_{2,\text{NLO}}^{ep}$  according to (8) results in  $r_{\text{NLO}}^{\text{QED}} = F_{2,\text{NLO}}^{ep,\text{QED}}/F_{2,\text{NLO}}^{ep}$ . Figure 2(a) demonstrates that ambiguities of standard NLO  $\overline{\text{MS}}$  analyses or additional QED contributions are comparable in size to NNLO contributions in the relevant medium and large  $x$ -region. Only in the smaller  $x$ -region around  $x = 0.2$ , the NNLO results are about 1% larger than the NLO ones. This difference, however, disappears in the DIS factorization scheme where  $r_{\text{NNLO}}^{\text{DIS}}$  and  $r_{\text{NLO}}^{\text{DIS}}$  are comparable and small (about 0.5%). We therefore conclude that the DIS scheme guarantees a better perturbative convergence than the commonly used  $\overline{\text{MS}}$  scheme, except in the very large  $x$ -region (where nonperturbative contributions are uncontrollable anyway). Unfortunately such minute effects are not testable with presently available precision data for non-singlet structure functions which have a typical uncertainty of about 10% in the small and large  $x$ -region.

The redundant  $\mathcal{O}(a^2)$  contribution to a NLO analysis, as discussed after (6), turns out to be marginal: repeating the NLO fit with the redundant term removed from  $F_{2,\text{NLO}}^{ep}$  in (6),

$$F_{2,\text{NLO}}^{ep,\text{rem}} = F_{2,\text{NLO}}^{ep} + a(a - a_0)C_{2,\text{NS}}^{(1)} R_1(a/a_0)^{-P_{\text{NS}}^{(0)}/\beta_0} v^+(Q_0^2) , \quad (17)$$

one obtains  $|r_{\text{NLO}}^{\text{rem}} - 1| = |F_{2,\text{NLO}}^{ep,\text{rem}}/F_{2,\text{NLO}}^{ep} - 1| \lesssim 0.001$  for all relevant values of  $Q^2$ .

Finally, the relevance of HT effects is illustrated in Fig. 2(b) where the ratios  $r_i^{\text{HT}} = F_{2,i}^{ep,\text{HT}}/F_{2,i}^{ep}$  for the different perturbative orders are shown, with the HT corrections incorporated according to (13). In general, for each perturbative order the fit results are *stable* with respect to different choices for the lower bound on  $Q^2$  in (13), i.e.,  $Q^2 \geq 4 \text{ GeV}^2$  and  $10 \text{ GeV}^2$  denoted by HT and HT(10), respectively. In particular the more relevant NLO and NNLO fit results are very similar. Despite the fact that these results are about twice as large as the ones without HT contributions in Fig. 2(a) throughout the whole  $x$ -region considered, they are still much smaller than present experimental uncertainties.

## 4 Conclusions

The significance of NNLO QCD contributions to the flavor non-singlet sector of  $F_2^{ep,d}(x, Q^2)$  has been studied as compared to uncertainties of standard NLO (and LO) analyses. NNLO corrections slightly improve the fits to presently available data and imply a better perturbative convergence in the DIS factorization scheme than in the commonly used  $\overline{\text{MS}}$  scheme. However, ambiguities of NLO fits such as the choice of a particular factorization scheme ( $\overline{\text{MS}}$  vs. DIS) and possible higher twist effects as well as QED  $\mathcal{O}(\alpha)$  contributions turn out to be comparable in size to NNLO (3-loop) contributions. In particular, nonperturbative higher twist effects play an important role in obtaining optimal fits (minimal  $\chi^2$ ) which turn out to be rather stable with respect to different choices of the lower bound on  $Q^2$ . Their contribution is about twice as large as purely perturbative uncertainties which are typically less than about 1%. We therefore conclude that the



rather minute NNLO QCD effects in the flavor non-singlet sector are not observable with present precision data for flavor non-singlet structure functions which have sizeably larger errors.

This work has been supported in part by the ‘Bundesministerium für Bildung und Forschung’, Berlin/Bonn.

## References

- [1] J. Blümlein, H. Böttcher, and A. Guffanti, *Nucl. Phys. B* (Proc. Suppl.) **135** (2004) 152
- [2] A.D. Martin et al., *Eur. Phys. J.* **C23** (2002) 73
- [3] R.S. Towell et al., E866 Collab., *Phys. Rev.* **D64** (2001) 052002
- [4] J. Blümlein and A. Vogt, *Phys. Rev.* **D58** (1998) 014020
- [5] W.L. van Neerven and A. Vogt, *Nucl. Phys.* **B568** (2000) 263
- [6] G. Altarelli, R.K. Ellis, and G. Martinelli, *Nucl. Phys.* **B143** (1978) 521; **B146** (1978) 544(E); *ibid.* **B157** (1979) 461
- [7] H. Spiesberger, *Phys. Rev.* **D52** (1995) 4936
- [8] S. Moch, J.A.M. Vermaseren, and A. Vogt, *Nucl Phys.* **B688** (2004) 101
- [9] J. Blümlein and S. Kurth, *Phys. Rev.* **D60** (1999) 014018
- [10] H. Georgi and H.D. Politzer, *Phys. Rev.* **D14** (1976) 1829
- [11] U.K. Yang and A. Bodek, *Phys. Rev. Lett.* **82** (1999) 2467; Proceedings of the 6th Int. Workshop on DIS and QCD, Brussels, 1998 (hep-ph/9806458)
- [12] S.I. Alekhin, *Phys. Rev.* **D68** (2003) 014002
- [13] A.C. Benvenuti et al., BCDMS Collab., *Phys. Lett.* **B223** (1989) 485; **B237** (1990) 592
- [14] M. Arneodo et al., NMC Collab., *Nucl. Phys.* **B483** (1997) 3
- [15] L.W. Whitlow et al., *Phys. Lett.* **B282** (1992) 475
- [16] C. Adloff et al., H1 Collab., *Eur. Phys. J.* **C30** (2003) 1

- [17] S. Chekanov et al., ZEUS Collab. *Eur. Phys. J.* **C21** (2001) 443
- [18] G. Parente, A.V. Kotikov, and V. Krivokhizhin, *Phys. Lett.* **B333** (1994) 190;  
A.L. Kataev et al., *Phys. Lett.* **B388** (1996) 179; **B417** (1998) 374
- [19] A.D. Martin et al., *Phys. Lett.* **B531** (2002) 216

Table 1: Parameter values of the QCD fits in various perturbative orders based on all non-singlet data for  $F_2^{ep,d}(x, Q^2)$ . The parameters of the input valence distributions refer to (15) and (16). The analysis for the DIS factorization scheme is based on (7) for NLO and on (11) for NNLO. The QED contribution to NLO is taken into account according to (8).

	Parameter			$\chi^2/\text{dof}$	$\alpha_s(m_Z^2)$ ( $\Lambda^{(4)}/\text{MeV}$ )
	$a_u$	$b_u$	$c_u$		
	$A_u$	$B_u$	$N_u$		
	$a_d$	$b_d$	$c_d$		
	$A_d$	$B_d$	$N_d$		
LO	0.574	3.290	0.823	0.98	0.128 (196.0)
	9.258	-7.164	1.790		
	0.600	4.952	0.100		
	-0.330	3.726	1.742		
NLO	0.600	3.364	0.667	0.93	0.112 (222.6)
	9.900	-8.504	1.521		
	0.600	5.163	0.181		
	3.294	8.303	0.542		
NLO DIS	0.600	3.004	0.855	0.91	0.113 (228.3)
	9.801	-9.010	2.101		
	0.581	4.797	0.878		
	-0.030	4.458	1.264		
NLO QED	0.600	3.361	0.667	0.93	0.112 (217.1)
	9.883	-8.496	1.523		
	0.599	5.161	0.186		
	3.223	8.037	0.555		
NNLO	0.600	3.571	0.599	0.89	0.111 (177.2)
	9.654	-6.810	1.309		
	0.600	5.209	0.323		
	4.060	4.870	0.657		
NNLO DIS	0.587	2.727	0.825	0.89	0.112 (187.2)
	9.644	-9.471	1.941		
	0.600	4.787	0.868		
	-2.004	6.046	1.421		

Table 2: As in Table 1 but including HT contributions as well according to (13) with the parameters  $(a, b, c)$  referring to (14). Fits using a lower bound  $Q^2 \geq 10 \text{ GeV}^2$  in (13) are denoted by HT(10), whereas HT refers to  $Q^2 \geq 4 \text{ GeV}^2$  as stated before (13). NLO and NNLO always refer to the  $\overline{\text{MS}}$  factorization scheme.

	Parameter			$\chi^2/\text{dof}$	$\alpha_s(m_Z^2)$ ( $\Lambda^{(4)}/\text{MeV}$ )
	$a_u$ $A_u$ $a_d$ $A_d$ $a$	$b_u$ $B_u$ $b_d$ $B_d$ $b$	$c_u$ $N_u$ $c_d$ $N_d$ $c$		
LO HT	0.600	3.218	0.397	0.82	0.118 (121.8)
	6.926	-4.208	1.021		
	0.582	4.882	0.712		
	7.205	-2.878	0.956		
	2.180	0.941	0.577		
LO HT (10)	0.600	3.167	0.422	0.88	0.126 (176.6)
	8.286	-5.214	0.942		
	0.597	4.985	0.750		
	6.163	-1.061	1.052		
	2.105	1.000	0.749		
NLO HT	0.600	3.368	0.508	0.83	0.104 (136.6)
	9.897	-8.215	1.104		
	0.600	5.383	0.222		
	4.905	9.563	0.467		
	2.198	1.468	0.303		
NLO HT (10)	0.600	3.429	0.522	0.90	0.106 (155.8)
	9.900	-7.786	1.126		
	0.598	5.507	0.190		
	2.383	9.824	0.642		
	2.313	1.740	0.284		
NNLO HT	0.600	3.571	0.519	0.83	0.103 (109.5)
	9.900	-7.086	1.116		
	0.566	5.425	0.302		
	5.816	9.475	0.441		
	1.695	1.104	0.432		
NNLO HT (10)	0.600	3.622	0.518	0.91	0.105 (124.9)
	9.898	-6.491	1.099		
	0.599	5.594	0.235		
	2.260	9.119	0.716		
	1.989	1.801	0.252		

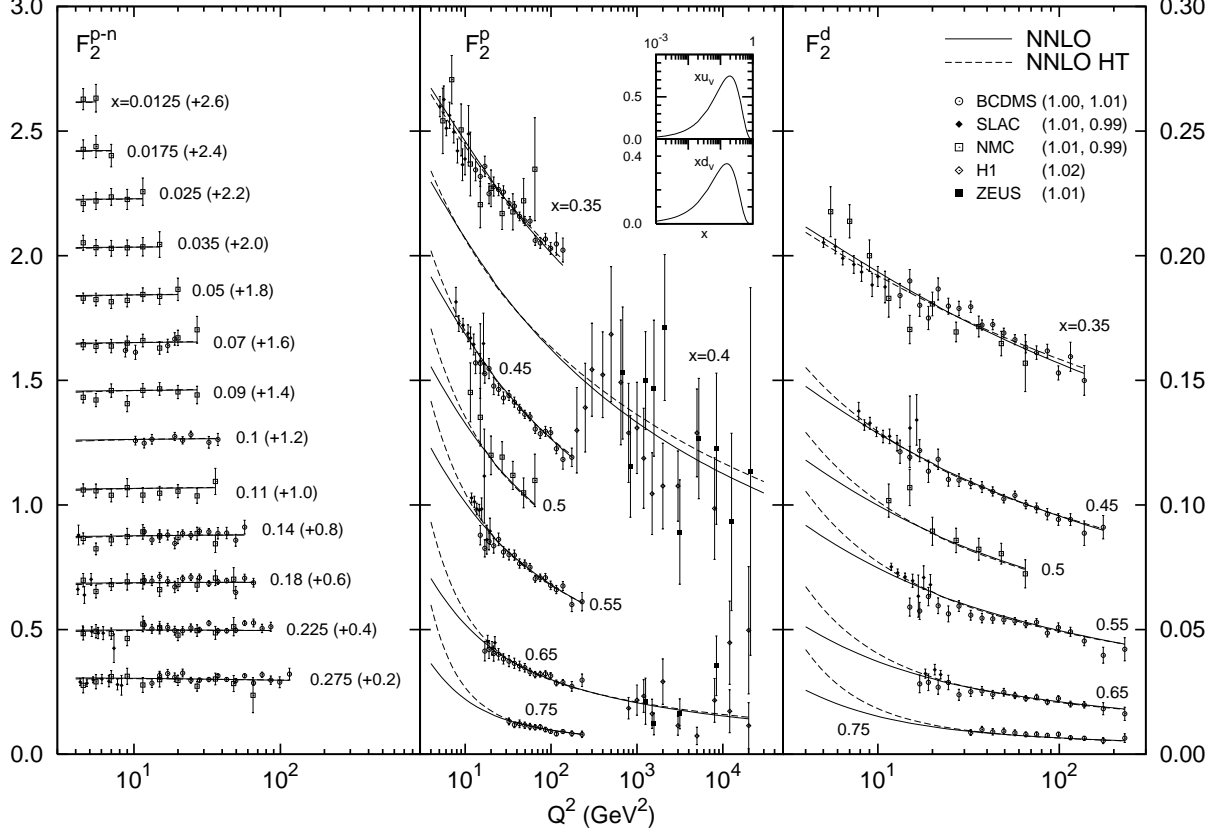


Figure 1: Comparison of our NNLO fits with all presently available flavor non-singlet data [13, 14, 15, 16, 17] used for our analysis. The higher twist (HT) contribution is taken into account according to (13) and (14). The NLO fits are very similar and practically indistinguishable from the ones shown. So is the NNLO HT(10) fit resulting from the cut  $Q^2 \geq 10 \text{ GeV}^2$ . The inset shows our NNLO input valence distributions at  $Q_0^2 = 4 \text{ GeV}^2$ . The scales on the left ordinate refer only to  $F_2^{p-n}$  where for each fixed value of  $x$  we have added the constant in brackets to  $F_2^{p-n}$ . The scales on the right ordinate refer to  $F_2^p$  and to  $F_2^d$ . The data sets are shown with their normalization factors in parentheses (first entry refers to  $F_2^p$ , second entry to  $F_2^d$ ) as obtained in the fit. The ZEUS data for  $F_2^p$  have been shifted to the right by 5 % in order to make their error bars distinguishable from the ones of the H1 data.

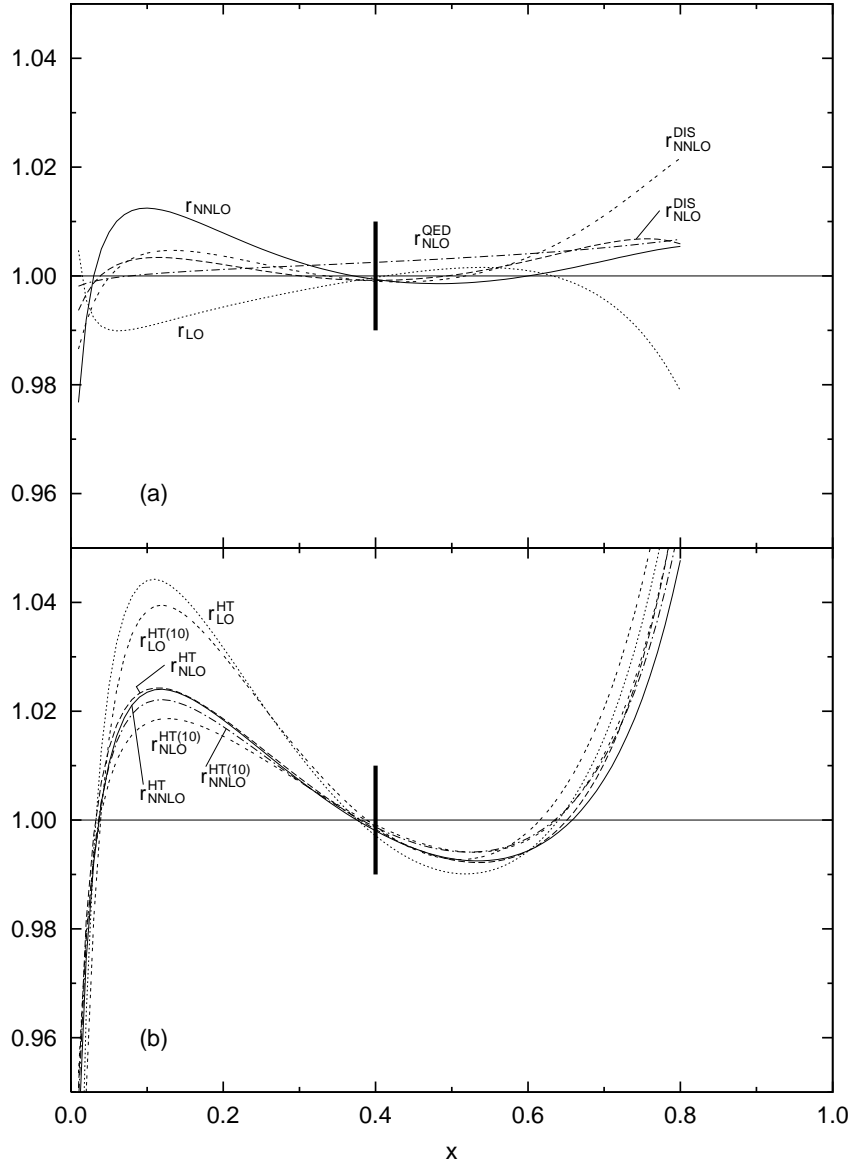


Figure 2: The size of perturbative (a) and nonperturbative (b) uncertainties encountered in various perturbative  $\alpha_s$ -orders of QCD analyses relative to our nominal NLO analysis of  $F_{2,\text{NLO}}^{ep}(x, Q^2)$  which always appears in the denominator of the ratios  $r$  as defined and discussed in the text. The HT contributions to the fits shown in (b) refer to the cut  $Q^2 \geq 4$  GeV<sup>2</sup>, whereas HT(10) refers to a cut  $Q^2 \geq 10$  GeV<sup>2</sup>. The typical relative experimental accuracy is illustrated at  $x = 0.4$  by the vertical bar ( $\pm 1\%$ ). At larger and smaller values of  $x$  the experimental error increases (e.g., the uncertainty is about  $\pm 2.5\%$  at  $x = 0.55$ , and  $\pm 10\%$  at  $x = 0.18$ ). All results are shown for  $Q^2 = 40$  GeV<sup>2</sup>, but the agreement with data at  $Q^2 = 4$  GeV<sup>2</sup> and  $Q^2 = 100$  GeV<sup>2</sup> is similar.